




Distinct Subsets of Noncoding RNAs Are Strongly Associated With BMD and Fracture, Studied in Weight-Bearing and Non-Weight-Bearing Human Bone

Kaare M Gautvik,^{1,2} Clara-Cecilie Günther,³ Vid Prijatelj,^{4,5} Carolina Medina-Gomez,⁵ Enisa Shevroja,⁵ Leila Heidary Rad,⁶ Mazyar Yazdani,⁶  Einar Lindalen,⁷ Haldor Valland,⁸ Vigdis T Gautvik,¹ Ole K Olstad,⁶ Marit Holden,³ Fernando Rivadeneira,⁵  Tor P Utheim,^{6,9,10,11} and Sjur Reppe^{1,2,6,9} 

¹Unger-Vetlesen Institute, Lovisenberg Diaconal Hospital, Oslo, Norway

²Department of Molecular Medicine, University of Oslo, Oslo, Norway

³Norwegian Computing Center, Oslo, Norway

⁴Department of Maxillofacial Surgery, Special Dental Care and Orthodontics, Erasmus MC, University Medical Center Rotterdam, Rotterdam, the Netherlands

⁵Department of Internal Medicine, Erasmus MC, University Medical Center Rotterdam, Rotterdam, the Netherlands

⁶Department of Medical Biochemistry, Oslo University Hospital, Oslo, Norway

⁷Orthopaedic Department, Lovisenberg Diaconal Hospital, Oslo, Norway

⁸Department of Surgery, Diakonhjemmet Hospital, Oslo, Norway

⁹Department of Plastic and Reconstructive Surgery, Oslo University Hospital, Oslo, Norway

¹⁰Department of Ophthalmology, Stavanger University Hospital, Oslo, Norway

¹¹Department of Ophthalmology, Sørlandet Hospital, Arendal, Norway

ABSTRACT

We investigated mechanisms resulting in low bone mineral density (BMD) and susceptibility to fracture by comparing noncoding RNAs (ncRNAs) in biopsies of non-weight-bearing (NWB) iliac ($n = 84$) and weight bearing (WB) femoral ($n = 18$) postmenopausal bone across BMDs varying from normal (T -score > -1.0) to osteoporotic (T -score ≤ -2.5). Global bone ncRNA concentrations were determined by PCR and microchip analyses. Association with BMD or fracture, adjusted by age and body mass index, were calculated using linear and logistic regression and least absolute shrinkage and selection operator (Lasso) analysis. At 10% false discovery rate (FDR), 75 iliac bone ncRNAs and 94 femoral bone ncRNAs were associated with total hip BMD. Eight of the ncRNAs were common for the two sites, but five of them (miR-484, miR-328-3p, miR-27a-5p, miR-28-3p, and miR-409-3p) correlated positively to BMD in femoral bone, but negatively in iliac bone. Of predicted pathways recognized in bone metabolism, ECM-receptor interaction and proteoglycans in cancer emerged at both sites, whereas fatty acid metabolism and focal adhesion were only identified in iliac bone. Lasso analysis and cross-validations identified sets of nine bone ncRNAs correlating strongly with adjusted total hip BMD in both femoral and iliac bone. Twenty-eight iliac ncRNAs were associated with risk of fracture (FDR < 0.1). The small nucleolar RNAs, RNU44 and RNU48, have a function in stabilization of ribosomal RNAs (rRNAs), and their association with fracture and BMD suggest that aberrant processing of rRNAs may be involved in development of osteoporosis. Cis-eQTL (expressed quantitative trait loci) analysis of the iliac bone biopsies identified two loci associated with microRNAs (miRNAs), one previously identified in a heel-BMD genome-wide association study (GWAS). In this comprehensive investigation of the skeletal genetic background in postmenopausal women, we identified functional bone ncRNAs associated to fracture and BMD, representing distinct subsets in WB and NWB skeletal sites. © 2020 The Authors. *Journal of Bone and Mineral Research* published by American Society for Bone and Mineral Research.

This is an open access article under the terms of the Creative Commons Attribution License, which permits use, distribution and reproduction in any medium, provided the original work is properly cited.

Received in original form July 26, 2019; revised form January 22, 2020; accepted January 26, 2020. Accepted manuscript online February 3, 2020.

Address correspondence to: Sjur Reppe, PhD, Oslo University Hospital, Ullevaal, Oslo, Norway. E-mail: sjur.reppe@medisin.uio.no

Additional Supporting Information may be found in the online version of this article.

The peer review history for this article is available at <https://publons.com/publon/10.1002/jbmr.3974>.

Journal of Bone and Mineral Research, Vol. 00, No. 00, Month 2020, pp 1–12.

DOI: 10.1002/jbmr.3974

© 2020 The Authors. *Journal of Bone and Mineral Research* published by American Society for Bone and Mineral Research

Postmenopausal osteoporosis is the most common disease in women above 50 years of age, leading to fragile bone and fractures even after mild skeletal trauma.⁽¹⁾ About 40% of all US white women will suffer at least one clinically apparent fragility fracture during their lifetime.⁽²⁾ The consequences of fractures, commonly occurring in the spinal vertebrae, wrists, and hip, pose a serious health risk to the patients and have a profound social and economic impact.⁽³⁾

High and low bone mineral densities (BMDs) are typically associated with strong and fragile bones, respectively. Reduced BMD leads to osteoporosis, defined by the World Health Organization (WHO) as a BMD of 2.5 standard deviations (SDs) or more below the young adult mean (T -score ≤ -2.5). BMD is highly heritable. Mothers with low BMD have children with significantly lower BMD more frequently than the general female population.⁽⁴⁾ Also, studies involving twins or kin relationships have demonstrated that individual variations in BMD are up to 80% genetically determined.^(5–7) A recent genomewide association study (GWAS),⁽⁸⁾ the most extensive so far, identified 518 loci accounting for approximately 20% of heel BMD variation. Some of the discrepancies between that GWAS and family studies may be explained by different epigenetics between osteoporotic and healthy subjects, as indicated by recent DNA methylation studies and difficulties detecting disease associated genetic variants due to minor contribution.^(9–11) MicroRNAs (miRNAs) are considered part of the possible epigenetic mechanisms contributing to osteoporosis risk, and their regulatory effect are heritable.^(12,13)

miRNAs are 19-nucleotide (nt)-long to 24-nt-long noncoding molecules that are distinct from, but related to, small interfering RNAs (siRNAs), and have been identified in a variety of organisms.⁽¹⁴⁾ They are transcribed from distinct genes and regulate the translation and/or degradation of specific messenger RNAs (mRNAs) or other transcripts, thereby modulating many critical cellular signaling pathways and functions.⁽¹⁴⁾ The miRBase database (release 22; Manchester University, Manchester, UK; <http://www.mirbase.org/>) contains well over 2500 mature human miRNAs.⁽¹⁵⁾ Despite the critical importance of miRNAs in the regulation of various cell functions, their role in osteoporosis has not yet been investigated in depth in well-characterized human bone.

In addition to miRNAs, thousands of other noncoding RNAs (ncRNAs) are transcribed from the human genome, and may regulate gene expression at transcription, RNA processing, and translation levels.⁽¹⁶⁾ These untranslated RNAs include small nucleolar RNAs (snoRNAs, SNORDs, SNORAs), most of which are pieces of introns (~70 nt) that have separate functions after being excised through exonucleolytic processing.⁽¹⁷⁾ The snoRNAs are essential for pre-ribosomal RNA (pre-rRNA) processing, catalyze nucleotide modifications, and may also serve to chaperone the correct RNA fold for rRNA processing and ribosome assembly.⁽¹⁸⁾

We aimed to establish a putative association of ncRNAs with BMD or fracture by performing global gene expression profiling of bone biopsies from postmenopausal white women with bone mass varying from healthy to osteoporotic with or without prior fragility fractures. mRNA levels vary considerably between weight-bearing (WB) spine and non-weight-bearing (NWB) iliac bone in the same individuals.^(19,20) To make the present study representative for different skeletal sites, we included NWB iliac and WB femoral bone where the most serious fractures occur.

Ethics statement

The study was approved by the Norwegian Regional Ethical Committee (REK no 2010/2539, Norway), all volunteers gave their written informed consent, and sampling and procedures were according to the Act of Biobanking in Norway.

Participants

The cohort of iliac bone donors was enlisted after completing a questionnaire that included questions on lifestyle factors and was deemed representative of the Oslo-based Norwegian ethnic female population aged 50 to 86 years. Nonrelated postmenopausal ethnic Norwegian women (50 to 86 years, $n = 300$) were recruited from the outpatient clinic of Lovisenberg Diaconal Hospital (Oslo, Norway). Of these, 177 were excluded from the study due to medication or diseases other than primary osteoporosis that are known to alter bone metabolism. Altogether, 100 women were enrolled in the study, and underwent transiliac bone biopsies of the anterior superior iliac crest. Eighty-four biopsies underwent gene expression analysis. The biochemical and physiological parameters of these women have been described.⁽¹¹⁾ Moreover, site-specific BMD was evaluated with Lunar Prodigy DEXA (GE Lunar, Madison, WI, USA) following the manufacturer's instructions. The precision of the instrument for measuring the lumbar spine (L_2 – L_4) and hip BMD was 1.7% and 1.1%, respectively.

Femoral bone intertrochanteric biopsies were obtained from postmenopausal women ($n = 18$) with a wide BMD range, ie, from healthy to osteoporotic, who were undergoing hip replacement surgery (Table 1). None of the participants had medication or diseases other than primary osteoporosis known to affect bone metabolism. Anthropometric data, including BMD, for each of the 18 donors are shown in Table S1.

Purification and quantification of ncRNAs

Total RNA was isolated from bone biopsies as described⁽¹¹⁾ and quality checked using Agilent BioAnalyzer (Agilent Technologies, Santa Clara, CA, USA).

For analysis of the iliac ncRNAs, total RNA (45 ng) was reverse-transcribed using Megaplex™ reverse transcription (RT) primersets A and B (Applied Biosystems, Foster City, CA, USA). TaqMan miRNA LDA Arrays A and B (Applied Biosystems) were used for profiling 758 different ncRNAs. The data were analyzed using SDS 2.3 software (Applied Biosystems, Foster City, CA, USA) and the comparative threshold cycle ($\Delta\Delta C_t$) method. We used a restricted mean of expressed miRNAs, and normalized between two plates with the same sample and performed a normalization across samples.

For mature miRNA and ncRNA microchip expression profiling of femoral bone intertrochanteric RNA, 300 ng total RNA was used for biotin labeling by a Genisphere FlashTag HSR kit (Genisphere, Hatfield, PA, USA) according to the manufacturer's protocol. Labeled miRNAs were hybridized to the GeneChip miRNA 4.0 Array (Affymetrix, Santa Clara, CA, USA). Affymetrix CEL files (containing probe intensities) were imported into Partek Genomics Suite software (Partek, St. Louis, MO, USA). Robust microarray analysis (RMA) was applied for normalization.

Lasso-selected femoral miRNAs from microarray data were validated using RT-PCR with Fast Advanced reagents (Thermo Fisher Scientific, Waltham, MA, USA), 384-well plates, and the

Table 1. Demographic, Clinical, and Laboratory Parameters of Femoral Bone Biopsy Donors

| Parameter | Average \pm SD | Laboratory reference ranges |
|---|-------------------|-----------------------------|
| Age (years) | 74.31 \pm 4.62 | NA |
| BMI (kg/m ²) | 23.40 \pm 2.85 | NA |
| Serum total-PTH (pmol/L) | 4.43 \pm 1.89 | 1.10–7.70 |
| Ionized Ca ²⁺ (mmol/L) | 1.20 \pm 0.03 | 1.15–1.35 |
| Serum Ca ²⁺ (corrected, mmol/L) | 2.38 \pm 0.08 | 2.15–2.51 |
| Serum-25(OH)vitD (nmol/L) | 52 \pm 20 | 30–110 |
| BGLAP (osteocalcin) (nmol/L) | 2.41 \pm 1.41 | <3.6 |
| CTX-1 (μ g/L) | 0.53 \pm 0.18 | <0.85 |
| Serum bone specific alkaline phosphatase (μ g/L) | 24.44 \pm 12.51 | 11.6–30.6 |
| BMD, total femoral neck (g/cm ²) | 0.77 \pm 0.10 | NA |
| BMD, total femoral neck (T-score) | –1.87 \pm 0.87 | NA |
| BMD, total femoral neck (Z-score) | –0.18 \pm 0.83 | NA |
| BMD, total femoral neck (BMI-adjusted Z-score) | 0.00 \pm 0.83 | NA |
| BMD, total body (g/cm ²) | 1.05 \pm 0.10 | NA |
| BMD, total body (T-score) | –0.73 \pm 1.32 | NA |
| BMD, total body (Z-score) | 0.86 \pm 1.22 | NA |
| BMD, total body (BMI-adjusted Z-score) | 0.00 \pm 1.21 | NA |

All biopsies were taken from the intertrochanteric region.

NA = not applicable; CTX-1 = carboxyterminal collagen crosslinks (bone resorption marker); Z-score = age adjusted T-score.

QuantStudio 12 K Flex Real-Time PCR System (Thermo Fisher Scientific, Waltham, MA, USA). miR-361-3p, miR-24-3p, and miR-107 were used as internal standards because microarray analysis showed that their levels were similar in all samples. The seven miRNAs in Table S5 resulted in measurable PCR products. The following assays were used (all from Thermo Fisher Scientific): miR-29c-3p: 479229_mir; miR-1-3p: 477820_mir; miR-1260b: 477886_mir; miR-484: 478308_mir; miR-3652: 480799_mir; miR-361-3p: 478055_mir; miR-24-3p: 477992_mir; miR-107: 478254_mir; miR-3921: 479742_mir; miR-92a-1-5p: 479205_mir; and miR-489-3p: 478130_mir.

Correlation studies

The Benjamini and Hochberg procedure⁽²¹⁾ was used for controlling the false discovery rate (FDR). The correlation coefficient was computed between variation in the expression levels of each mature miRNA/ncRNA expressed in 95% of the biopsies and the BMD for all subjects ($n = 84$). For each RNA, the null-hypothesis of zero correlation was tested against the two-tailed alternative hypothesis. Correlation coefficients were computed for BMD adjusted for age (Z-score) and BMI, first by regressing the BMD Z-score on BMI values (with intercept), and then defining the residuals as the BMI-adjusted Z-scores.

Lasso analysis and cross-validation

In addition to identifying the individual transcripts showing significant correlation with BMD, we also selected a set of transcripts that together accounted for a substantial percentage of the BMD variation. The set was selected using the Lasso method

for variable selection and shrinkage in regression models.⁽²²⁾ Cross-validation was performed to estimate the penalty parameter of the Lasso method. The Lasso analysis, including the cross-validation step, was performed for BMD Z-scores adjusted for BMI in total hip, femoral neck, and spine (L₂–L₄) using the R-package lars⁽²²⁾ (<http://cran.r-project.org/web/packages/lars/index.html>)⁽²³⁾ and the R-package glmnet (<https://cran.r-project.org/web/packages/glmnet/index.html>). The R^2 value for each estimated model was also computed. To compare the performance of the selected sets of transcripts to a random selection of transcripts, the R^2 value of an ordinary least squares regression with the selected set was compared to the R^2 values of an ordinary least squares regression for each of 10,000 randomly selected sets of the same. The p value was calculated as the proportion of the random sets with a higher R^2 value than the Lasso-selected set.

Gene enrichment analysis

We used mirPath v.3 in DIANA TOOLS (<http://diana.imis.athena-innovation.gr/DianaTools/index.php>),⁽²⁴⁾ which has high sensitivity and relatively high precision,⁽²⁵⁾ to identify overrepresented pathways among the iliac and femoral bone miRNAs correlated with adjusted total hip BMD at 10% FDR (Table 4).

Calculation of fracture associated iliac bone ncRNAs

To test whether the expressions of the transcripts were related to fracture, a logistic regression model was fitted for each of the 303 transcripts from iliac bone, with fracture (yes/no) as the response variable and transcript, age, and BMI as explanatory variables. The Wald test p values were corrected for multiple testing by using the Benjamini and Hochberg procedure.⁽²¹⁾ In this analysis, 47 iliac bone donors without fracture and 36 with previous fracture were included. Out of the 36, 23 had at least one vertebral fracture and 27 had at least one nonvertebral fracture (wrist or femoral neck). Associations with fracture were performed only for iliac bone donors because only two of the femoral bone donors did not have fracture.

Cis-eQTL (expressed quantitative trait loci) analysis of iliac bone samples

Genomewide genotyping of the iliac bone donors was performed using the Affymetrix Axiom Biobank Genotyping Array (Affymetrix, Santa Clara, CA, USA) (~700,000 SNPs assessed),⁽²⁶⁾ followed by imputation to the haplotype reference panel (HRC 1.0). SNPs with minor allele frequency (MAF) > 0.05 and imputation quality (R^2) > 0.3 were considered for further analysis. Combining the available genotyped patient data and iliac bone ncRNA expression data of patients yielded data of 77 patients in total. We then used a two-step approach to assess the association of SNPs with the expression of each ncRNA. First, using linear models we adjusted the ncRNA expression for either age or age and BMI, and then defined the model residuals as either age-adjusted RNA expressions or age- and BMI-adjusted RNA expression. These model residuals were scaled using zero mean unit variance standardization. Second, we performed cis-eQTL analyses, using the Rvtests software package with single variant tests,⁽²⁷⁾ for each adjusted ncRNA expression. SNPs within 500 kilobases (kb) of the ncRNA transcription start or termination sites were surveyed. Values of p of association were adjusted for multiple testing (FDR < 0.05).

Verification of expression of relevant miRNAs in osteoblasts/osteocytes

About 95% of bone cells constitute osteoblasts/osteocytes, but the bone biopsies also contained bone marrow, including non-bone cell types. Thus, it was necessary to examine whether the BMD associated miRNAs were expressed in osteoblasts/osteocytes. For this purpose we took advantage of data from De-Ugarte and colleagues,⁽²⁸⁾ who performed microarray profiling of primary osteoblasts obtained from bone biopsies taken during knee replacement due to osteoarthritis ($n = 4$, NCBI GEO repository, accession number GSE74211).

Results

Cohorts and experimental strategy

We used bone biopsies from two cohorts of postmenopausal women (age range, 50 to 86 years), and statistical analyses were carried out as outlined in Fig. 1.

Demographic, clinical, and laboratory parameters of the iliac bone donors

Demographic, clinical, and laboratory parameters of the iliac bone donors, have been described.⁽¹¹⁾ Briefly, the mean \pm SD age and BMI of the 84 subjects were 64.6 ± 9.6 years and 24.2 ± 3.6 kg/m², respectively. They had a wide range of BMD of

the spine (L₂–L₄; T -score range: -6.2 to 2.9), femoral neck (-4.1 to 1.3), and total hip (-4.1 to 2.0), spanning osteoporotic to normal BMD. All participants had normal clinical, biochemical, and nutritional status. The mean levels of parathyroid hormone (PTH), vitamin K, Ca²⁺, phosphate, and 25(OH) vitamin D, as well as the bone remodeling parameters osteocalcin, pyridinoline cross-linked carboxyterminal telopeptide of type I collagen (1CTP) and bone-specific alkaline phosphatase were all within normal reference ranges.⁽¹¹⁾ Quantitative histomorphometry in an additional seven women (T -score total hip range: -3.3 to 1.1) showed no change in osteocyte number between normal and osteoporotic trabecular bone from iliac crest.⁽¹¹⁾

Demographic, clinical and laboratory parameters of the femoral bone donors

Data on the femoral bone donors are presented in Table 1. This cohort consisted of postmenopausal women ($n = 18$) with a wide range in BMD, from healthy to osteoporotic, undergoing hip replacement surgery.

Identification of BMD-associated ncRNAs in iliac or femoral bone biopsies

Table 2 summarizes significant correlations found between gene expression signal strength of ncRNAs originating from either iliac or femoral bone and BMD variation in the same donors. For iliac bone, 303 ncRNAs were detected in >95% of the samples and

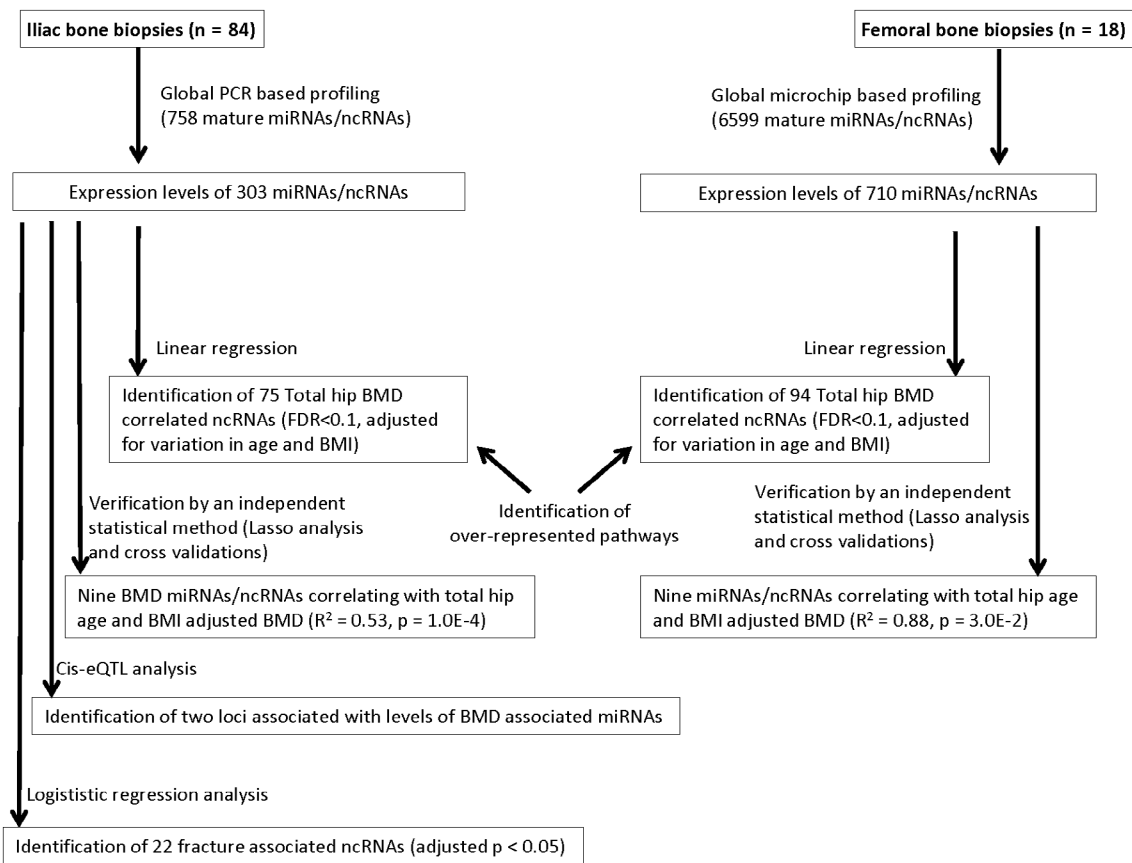


Fig. 1. Overview of cohorts, methods, and biostatistics with summary results.

Table 2. Number of ncRNAs from Iliac or Femoral Bone Correlating With Total BMD at Different Sites

| Parameter | Unadjusted $p < .05$ | FDR 1% | FDR 5% | FDR 10% |
|--|----------------------|--------|--------|---------|
| A. Number of BMD-associated ncRNAs from iliac bone | | | | |
| Total hip | 90 | 36 | 58 | 75 |
| Femoral neck | 83 | 11 | 52 | 67 |
| L ₂ –L ₄ | 67 | 0 | 17 | 33 |
| B. Number of BMD-associated ncRNAs from femoral bone | | | | |
| Total hip | 186 | 0 | 0 | 94 |
| Femoral neck | 69 | 0 | 0 | 0 |
| L ₂ –L ₄ | 220 | 0 | 0 | 36 |

The table shows number of BMD correlated ncRNAs derived from iliac bone (A) and femoral bone (B) after correction for variation in age and BMI at indicated sites with unadjusted p value and with different levels of FDR. BMI = body mass index.

were used for all remaining statistical analyses. For femoral bone, analyzed by microarrays, ncRNA transcripts with \log_2 signal <5 across all samples were omitted.

In iliac bone, when accounting for multiple testing, applying FDRs of varying stringency (1%, 5%, 10%), 36, 58, and 75 transcripts, respectively, correlated with BMI-adjusted total hip Z-score (age adjusted T -score) (Table 2). Table 2 also shows the corresponding numbers for the femoral neck and L₂–L₄ BMI-adjusted Z-scores. In femoral bone, no ncRNAs were identified for total hip BMI-adjusted Z-score at 1% or 5% FDR, but 94 were identified at 10% FDR. Table 2 shows that in femoral bone as well as in iliac bone, more transcripts were correlated to BMD at the total hip as compared to BMD at the femoral neck and the lumbar regions after adjustment for FDR. The correlated transcripts identified for the different skeletal sites at $\leq 10\%$ FDR are presented in Table S2 (iliac bone) and Table S3 (femoral bone). The relative amounts of the 36 iliac ncRNAs at 1% FDR are presented in Fig. S1.

The Venn diagram in Fig. 2 shows that, out of 94 femoral bone and 75 iliac bone ncRNAs associated with total hip BMD (FDR $\leq 10\%$), eight were common and represented miRNAs (Fig. S2). Interestingly, five of the femoral miRNAs showed a positive correlation to total hip BMD, whereas in iliac bone they were inversely correlated (miR-27a-5p, miR-28-3p, miR-328-3p, miR-409-3p, and miR-484), indicating an unexpected difference between the two sites.

Lasso analysis

Lasso analysis is a regression-based analytical method commonly used when variables outnumber samples.^(29,30) We used Lasso analysis as a separate independent statistical method on both cohorts of bone donors to identify sets among all detected transcripts that would explain a high proportion of BMD. The Lasso analysis selected nine ncRNAs in both iliac and femoral bone. The degree of explained total hip BMD variation after adjustment for age and BMI was calculated from an ordinary least squares regression model with the selected ncRNAs, and was 53% ($R^2 = 0.53$, $p = 1.0E-4$) and 88% ($R^2 = 0.88$, $p = 3.0E-5$) for iliac bone and femoral bone, respectively (Table 3). Absence of ncRNAs selected for femoral ncRNAs associated with total femoral neck and spine is probably due to weaker associations and few samples, because the number of selected variables depends on sample size.

Because it is possible that the Lasso-selected sets of ncRNAs could explain a large proportion of the variation in BMD just by

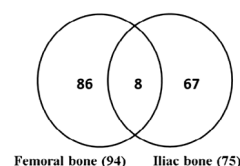


Fig. 2. Common BMD-associated ncRNAs between iliac and femoral bone adjusted for variation in age and BMI. The Venn diagram shows numbers of common and site-specific ncRNAs in iliac and femoral bone at 10% FDR. The eight common transcripts are presented in Fig. S2.

Table 3. Statistical Parameters for the Lasso Selected Sets of ncRNAs in Iliac and Femoral Bone

| Parameter | Total hip | Total femoral neck | Spine (L ₂ –L ₄) |
|---------------------------------|-----------|--------------------|---|
| Results for iliac bone ncRNAs | | | |
| R^2 (number of ncRNAs) | 0.53 (9) | 0.44 (7) | 0.87 (33) |
| p value | 1.0E–04 | 1.0E–04 | 1.0E–04 |
| Average R^2 | 0.26 | 0.20 | 0.49 |
| Results for femoral bone ncRNAs | | | |
| R^2 (number of ncRNAs) | 0.88 (9) | | |
| p value | 3.0E–02 | | |
| Average R^2 | 0.74 | | |

R^2 values were calculated for ordinary least squares regression models as described in Subjects and Methods. In parentheses, the number of ncRNAs selected by the Lasso analysis and used for calculation of R^2 values. As control, average R^2 and p values were calculated from 10,000 random sets of the same size as those selected by Lasso for the respective anatomical sites. Lasso did not select femoral ncRNAs associated with total femoral neck nor spine. This is probably due to weaker associations and because of few samples as the number of selected variables is dependent on sample size.

chance, we compared the results ($R^2 = 0.53$ and $R^2 = 0.88$) to the R^2 of the ordinary least squares regressions for 10,000 randomly selected sets of ncRNAs with set sizes of nine. On average, the random sets resulted in $R^2 = 0.26$ and $R^2 = 0.74$ for iliac bone and femoral bone, respectively, which is clearly lower than what was found as variance explained of total hip BMD for the initial

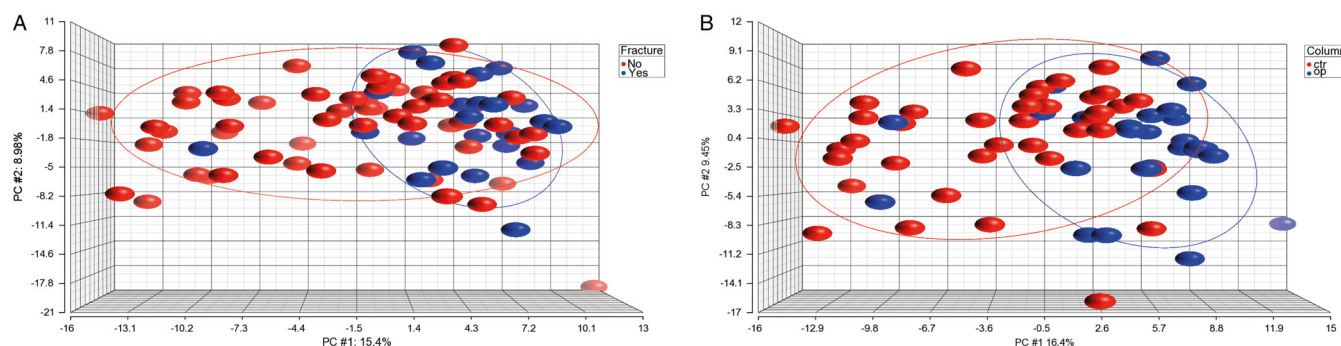


Fig. 3. PCA of iliac bone donors. (A) Distribution of all iliac bone donors with any fracture (blue balls) versus those without (red balls). (B) Distribution of osteoporotic iliac bone donors (T -score ≤ -2.5) versus controls (T -score > -1). PCA = principal component analysis.

Lasso-selected sets. None of the random sets for iliac bone (total hip, total femoral neck, L_2 – L_4) had R^2 as large as the sets identified by Lasso analysis.

Seven of the nine Lasso-identified iliac bone ncRNAs were among the 36 that were significantly correlated ($<1\%$ FDR) to adjusted total hip BMD (Tables S2 and S4A). Furthermore, eight of the nine Lasso-identified femoral ncRNAs were among the set of 94 ncRNAs correlating ($<10\%$ FDR) to total hip BMD adjusted Z-score (Tables S3 and S4B). Table S4A lists all of the selected Lasso-identified iliac ncRNAs for age- and BMI-adjusted BMD for total hip ($n = 9$), total femoral neck ($n = 7$), and L_2 – L_4 ($n = 33$). Table S4B shows the corresponding Lasso-identified femoral bone ncRNAs. Notably, Lasso identified no common ncRNAs between iliac and femoral bone.

Femoral bone BMD-associated miRNAs were also verified by PCR (Table S5), showing correlation r values in the same direction as found in Lasso analysis, although with p values $>.05$, possibly due to the limited number of samples. Although the nine femoral ncRNAs identified by Lasso and microarray analysis could explain 88% ($R^2 = 0.88$) of the variation in adjusted total hip BMD, PCR and multiple linear regression analyses of seven of these femoral bone ncRNAs could explain 44% ($R^2 = 0.44$) of the variation in the adjusted total hip BMD, thus supporting microarray and Lasso findings. Relative levels of the PCR tested miRNAs are presented in Fig. S3.

Identification of fracture associated ncRNAs

Using a logistic regression model (Subjects and Methods) we identified 29 ncRNAs to be associated with any previous fracture in the cohort of iliac bone donors at adjusted $p < .05$. The top-most fracture associated ncRNAs (adjusted $p < .1$) are listed in Table S6. Out of the 36 women with fracture 23 had at least one vertebral compression fracture.

Of the 29 fracture-associated iliac miRNAs, only miR-16-1-3p and miR-23a-3p were not among the ncRNAs correlated to BMD in Table S2. To test whether they were associated with hip bone geometry they were correlated to hip structure parameters in $n = 80$ of the same bone donors. Hip bone geometry in these donors has been described.⁽³¹⁾ Interestingly, miR-16-1-3p showed nominally significant correlation with neck shaft angle ($r = -0.22$, $p = .050$) and section modulus of the femoral neck ($r = 0.22$, $p = .050$).

The PCA plot (Fig. 3A) is based on all detected iliac ncRNAs, and indicates that iliac bone donors with fracture has a common ncRNA expression profile that at least partly separates them from donors without fracture. The woman representing the leftmost blue outlier ball had nonvertebral as well as vertebral fractures, thus suggesting an underlying disease, although all biochemical markers were normal. The PCA plot in Fig. 3B is also based on all iliac ncRNAs and shows grouping of donors with T -score ≤ -2.5 (blue balls) as compared to donors with normal BMD (T -score > -1 , red balls).

Functional annotation clustering of predicted miRNA targets in iliac and femoral bone

Gene enrichment analysis showed that the majority of the identified pathways are specific to either iliac or femoral bone (Table 4). As expected, extracellular matrix (ECM)-receptor interaction, being central in bone metabolism, was the second most significantly enriched pathway at both skeletal sites. Moreover, fatty acid metabolism was more prominent in iliac bone than in femoral bone.

Cis-eQTL analysis of iliac bone samples

DNA from the iliac bone biopsies has previously undergone gene profiling using the Affymetrix UK Biobank Axiom Array.⁽²⁶⁾ To evaluate whether SNPs within a 1-megabyte (MB) window of the ncRNA-encoded regions influenced the ncRNAs levels, we performed two cis-eQTL analyses, adjusting for age and for age and BMI (Subjects and Methods). At $q < 0.05$, rs12187909 was associated with miR-449b-5p ($p = 4.14E-5$) and rs74918612 associated with miR-331-3 ($p = 7.59E-4$). The former came out as suggestively correlated when adjusting ncRNA expressions only for age, and the latter when adjusting ncRNA expressions for age and BMI (Table 5). Tables S7 to S11 include detailed results from the cis-eQTL analysis, including all ncRNA-associated SNPs adjusted for age or age and BMI with q values. These tables also present p values for the same SNPs from the GWAS by Morris and colleagues⁽⁸⁾ on estimated heel bone mineral density (eBMD).

Figures S4 and S5 show the squared coefficients of correlation (R^2) between different SNPs, as curated from the cis-eQTL analysis results with age as predictor, where their respective q values were both <0.1 for miR-449b-5p and miR-331-3p.

Table 4. Overrepresented Biochemical and Cellular Signaling Pathways Predicted to be Affected by BMD Associated miRNAs in Iliac and Femoral Bone

| KEGG pathway | <i>p</i> | Genes (<i>n</i>) | miRNAs (<i>n</i>) |
|---|----------|--------------------|---------------------|
| Iliac bone | | | |
| Fatty acid biosynthesis ¹ | <1E–325 | 5 | 4 |
| ECM-receptor interaction ² | <1E–325 | 47 | 12 |
| Mucin type O-Glycan biosynthesis ¹ | <1E–325 | 19 | 16 |
| Amebiasis ² | 8.86E–10 | 21 | 4 |
| Fatty acid metabolism ¹ | 2.44E–08 | 16 | 7 |
| Glioma ² | 9.50E–08 | 44 | 13 |
| Proteoglycans in cancer ² | 2.27E–05 | 106 | 13 |
| Signaling pathways regulating pluripotency of stem cells ¹ | 8.13E–05 | 71 | 8 |
| Glycosaminoglycan biosynthesis – heparan sulfate/heparin ¹ | 2.42E–04 | 9 | 10 |
| Focal adhesion ¹ | 6.62E–03 | 100 | 7 |
| Lysine degradation ² | 1.05E–02 | 18 | 9 |
| PI3K-Akt signaling pathway ¹ | 1.32E–02 | 131 | 7 |
| Amphetamine addiction ¹ | 1.81E–02 | 32 | 13 |
| Femoral bone | | | |
| Prion diseases ³ | <1E–325 | 1 | 2 |
| ECM-receptor interaction ² | <1E–325 | 31 | 7 |
| Metabolism of xenobiotics by cytochrome P450 ³ | 1.46E–06 | 14 | 9 |
| Proteoglycans in cancer ² | 1.85E–04 | 101 | 12 |
| Lysine degradation ² | 2.15E–03 | 17 | 10 |
| Hippo signaling pathway ³ | 4.21E–03 | 71 | 11 |
| Glycosphingolipid biosynthesis – lacto and neolacto series ³ | 5.48E–03 | 10 | 8 |
| Morphine addiction ³ | 1.20E–02 | 31 | 7 |
| Amebiasis ² | 1.63E–02 | 20 | 2 |
| Thyroid hormone synthesis ³ | 1.86E–02 | 9 | 6 |
| Glioma ² | 3.52E–02 | 33 | 8 |

The table shows predicted affected KEGG pathways at *p* values <.05 using DIANA – mirPath v.3 with the following settings: pathways intersection, FDR correction (conservative stats: left unchecked).

¹ Pathways specific to iliac bone.

² Pathways common to iliac and femoral bone.

³ Pathways specific to femoral bone.

Table 5. Cis-eQTL Analysis on Levels of Iliac Bone ncRNAs

| Locus area (containing SNPs associated with indicated miRNAs at <i>q</i> value <0.05) | | | | | Locus previously associated with BMD ⁽⁸⁾ | Correlation with total hip <i>T</i> -score (<i>r</i>) |
|---|------------|-----------|----------|-------------|---|---|
| miRNA | Chromosome | POS start | POS end | Covariate | | |
| miR-331-3p | 12 | 95364009 | 96149571 | Age and BMI | Yes ⁽⁸⁾ | –0.58 |
| miR-449b-5p | 5 | 54651510 | 54896300 | Age | No | –0.35 |

Details of the Cis-eQTL analysis are found in the Supplemental Data. POS = Position.

Discussion

We present the hitherto most comprehensive study characterizing functional ncRNA expression patterns in NWB iliac and WB femoral bone in well-characterized cohorts of osteoporotic and healthy postmenopausal white women. Comparisons between the BMD-correlated ncRNAs expressed at the two sites revealed major differences with minor overlap and distinct, overrepresented signaling pathways. Lasso analysis of the bone ncRNAs enabled the identification of small sets of ncRNAs explaining a significant proportion of BMD variation measured at different skeletal site. We also identified miRNAs associated with fracture or SNPs.

The common pathways affected by BMD-associated miRNAs in both iliac and femoral bone include that for ECM-receptor interaction and proteoglycans in cancer, both of which are obviously important in all types of bone. The three other common pathways, Amebiasis, Glioma, and Lysine degradation, have no obvious function in bone and may be the result of miRNA targets being common to several functional pathways. For example, the glioma pathway includes miRNA targets such as mammalian target of rapamycin (*MTOR*), platelet-derived growth factor receptor alpha (*PDGFRα*), and epidermal growth factor (*EGF*), which have established functions in bone metabolism.^(32–34) The ECM-receptor interaction pathway involves interactions between various cell-associated integrins

and matrix collagens which are central actors in bone metabolism. This pathway overlaps with the focal adhesion pathway, ranked tenth in iliac bone but ranked as not significant in femoral bone. Notably, the focal adhesion pathway is linked to the Wnt pathway, which is central to bone metabolism.⁽³⁵⁾ Other iliac bone pathways related to bone matrix include that for mucin O-glycan biosynthesis and glycosaminoglycan biosynthesis, which are of obvious relevance to BMD.

The pathways specific to iliac bone also include that for fatty acid biosynthesis and fatty acid metabolism. It is well known that bone marrow stem cells (BMSCs) tend to differentiate toward adipocytes rather than osteoblasts in osteoporotic bone,⁽³⁶⁾ and an inverse association between BMD and marrow adipose tissue has been demonstrated in different populations.⁽³⁷⁾ A larger study with higher power might be able to detect these pathways in WB femoral bone.

It is unclear how several of the identified pathways targeted specifically by femoral bone miRNAs are associated with BMD, with the exception of the Hippo signaling pathway. The Hippo signaling pathway is important for stem cell function, bone development, and bone remodeling via interactions with, eg, the transforming growth factor beta (TGF- β)/SMAD pathway, Wnt signaling, and the transcription factor RUNX2 (RUNX family transcription factor 2).⁽³⁸⁾ Supporting the relevance of these findings in bone tissue, 22 of 46 ncRNAs have been shown to be important for bone cell differentiation and function in cell and animal models (Table S5).

Figure S2 shows that some ncRNAs were positively correlated to BMD when expressed in WB bone, but inversely when expressed in NWB bone. Transcript levels have previously been shown to vary widely between WB and NWB bone. For example, the transcription factor ZIC1 was shown to be expressed 200-fold higher in male bone biopsies from WB lumbar spine as compared to NWB iliac crest in the same donors.⁽²⁰⁾ In the same study, more than 4000 genes were identified as differentially expressed between the two sites. Thus, the observed inverse associations may reflect another aspect of differential bone metabolism in WB and NWB bone.

We searched the literature to identify whether the total hip BMD associated ncRNAs from iliac bone and femoral bone have been experimentally shown to impact bone metabolism. The relevant studies are summarized in Table S12. Briefly, 22 of the 46 ncRNAs have been associated with bone metabolism and/or osteogenic cell differentiation; eg, miR-92a-1-5p influences osteogenic differentiation in vitro by regulating β -catenin⁽³⁹⁾ and reduces body and skull length in miR-92a^{-/-} mice⁽⁴⁰⁾ and inhibition of miR-92a-1-5p enhances fracture healing.⁽⁴¹⁾ The miR-15a-5p is part of the deleted in lymphocytic leukemia 2 (*DLEU2*) gene, which is highly correlated to BMD in postmenopausal women⁽¹¹⁾ and mice (own results unpublished). In addition, miR-149-5p may be of clinical importance, because polymorphisms within its encoded primary RNA sequence have been associated with vertebral fractures in postmenopausal Korean women.⁽⁴²⁾ Most of the miRNAs in Table S7 affect functions attributed to bone cell differentiation and mineralization involving both osteoblast and osteoclast lineages confirming their skeletal functionality.

The bone biopsies contain also non-bone cells, and it may be argued that some of the BMD-associated ncRNAs are not originating from bone cells. However, all but five of the 36 topmost femoral bone miRNAs significant at 10% FDR (Table S3) when correlated to BMI-adjusted total hip Z-score were also produced in cultured differentiated normal human osteoblasts (publicly available data described by De-Ugarte and colleagues⁽²⁸⁾; not

shown). Notably, the five miRNAs not found were not covered by the GPL20999 miRCURY LNA miRNA Array used to profile the osteoblast miRNAs.

Notably, separate sets of small nucleolar RNAs (SNORAs, SNORDs, or snRNAs) from iliac and femoral bone were correlated with BMD. In iliac bone, SNORD44 and SNORD48, which direct 2'-O-ribose methylation of 18S rRNA and 28S rRNA, respectively,^(43–45) were negatively correlated with BMD, whereas 28SrRNA was positively correlated with BMD (Table S2). Interestingly, 28SrRNA showed an inverse correlation with SNORD44 and SNORD48 ($r = -0.57$ and $r = -0.81$; $p = 1.2E-8$ and $p = 1.0E-15$, respectively). rRNA methylation is important for rRNA processing and function, and failure in rRNA methylation has been linked to several diseases.⁽⁴⁶⁾ The connection between BMD and rRNA levels is supported by the identification of functional RUNX2 binding sites within DNA repeats encoding rRNA⁽⁴⁷⁾ and the fact that RUNX2 suppresses rRNA gene transcription during osteoblast lineage progression.^(48,49) In iliac bone, 28S rRNA was significantly correlated to nearly all BMD-correlated miRNAs at 1% FDR (not shown). This may be due to the expansion segments of 28S rRNA, which have been suggested to constitute an important component of miRNA balance by binding and decreasing ("sponging") the availability of GC-rich miRNAs and thereby aid the conservation of GC-rich mRNAs.⁽⁵⁰⁾ Iliac RNU11 (RNA, U11 small nuclear) was positively correlated to BMD and has functions such as 5' splice site recognition at constitutive splicing, activation of U2-dependent alternative splicing, and regulating the U12-dependent spliceosome,⁽⁵¹⁾ indicating that altered splicing may be an important mechanism affected in osteoporosis.

In femoral bone at 10% FDR, another set of total hip BMD-correlated nucleolar RNAs was found, consisting of seven SNORDs catalyzing 2'-O-ribose methylation of rRNA and five SNORAs guiding rRNA pseudouridylation⁽⁵²⁾ (Table S3). The majority of snoRNAs are encoded in the introns of host genes,⁽⁵³⁾ and their expression levels are thus correlated with their host gene transcripts and regulated similarly. Furthermore, crosslinking studies have indicated that SNORDs/SNORAs can also modify mRNAs,⁽⁵⁴⁾ thereby possibly affecting the level of bone cell transcripts related to skeletal metabolism.

However, it is striking that several miRNAs that promote osteogenesis/osteoblastogenesis in in vitro experiments are inversely correlated to BMD. This, may seem counterintuitive at first and apply, eg, to the following iliac bone miRNAs: miR-22-3p,^(55–57) miR-31-5p,⁽⁵⁸⁾ miR-124-3p,^(59–62) miR-34a-5p,⁽⁶³⁾ miR-378a-3p,^(64–66) miR-27a-5p,^(67–71) miR-342-3p,^(72,73) miR-15b-5p,^(74,75) and miR-10a⁽⁷⁶⁾; the femoral bone miRNAs: miR-23b-3p,⁽⁷⁷⁾ and miR-181a-2-3p^(78–80); as well as miR-48a-3p from both femoral and iliac bone.⁽⁵⁸⁾ We suggest that changes in these miRNAs compensate for further bone loss. Previously we showed that *SOST* (sclerostin) gene transcription and serum sclerostin levels were positively correlated to BMD and were reduced in postmenopausal osteoporosis.⁽⁸¹⁾ These changes could be attributed to hypermethylation of the *SOST* promoter in the same cohort of iliac bone patients, a possible epigenetic regulation aiming to balance the well-known sclerostin inhibition of osteoblast bone formation.⁽¹⁰⁾

It should be noted that several of the miRNAs with a positive correlation with BMD also promote osteogenesis in vitro; eg, iliac bone miRNAs: miR-29a-3p,^(59,82–86) miR-28-5p,⁽⁸⁷⁾ miR-181a-5p,^(78–80) and miR-27a-5p^(67–71); femoral bone miRNAs: miR-335-5p,⁽⁸⁸⁾ miR-194-5p,⁽⁸⁹⁾ and miR-378a-5p,^(64–66) as well as miR-29c-3p (in femoral and iliac bone).⁽⁹⁰⁾ It is noticeable and of potential importance that most of the osteogenesis-

associated miRNAs inversely correlated to BMD are found in iliac bone, whereas most of the osteogenic miRNAs positively correlated to BMD, are detected in femoral bone.

Of the 29 fracture-associated ncRNAs (Table S6), it is striking that all but one (miR-181a-5p) increase risk of fracture at increased expression levels. Furthermore, miR-16-1-3p (adj. $p = .0356$) and miR-23a-3p (adj. $p = .0745$) were not among any of the ncRNAs correlated to BMD in Table S2, and may therefore be particularly associated with structure, as also indicated by the association of miR-16-1-3p with hip structure.

Because of the limited availability of human bone biopsies, only a few similar, smaller ncRNA profiling studies have been performed, and none has been performed on NWB iliac bone. In a smaller study De-Ugarte and colleagues⁽²⁸⁾ determined that miR-320a and miR-483-5p are increased in osteoporotic bone. miR-320a was replicated in the present study, whereas miR-483-5p was detected but did not reach significance. A more comprehensive study by Seeliger and colleagues⁽⁹¹⁾ indicated that miR-21, miR-23a, miR-24, miR-25, miR-100, and miR-125b are upregulated in osteoporosis using unadjusted statistics. They were also detected in the femoral bone biopsies in the present study, but did not reach significance when correlated to BMD adjusted for variation in age and BMI. Garmilla-Ezquerria and colleagues⁽⁹²⁾ compared expression of 760 miRNAs in explanted osteoblasts from the femoral heads from patients with osteoporotic hip fractures and used patients with osteoarthritis as surrogate controls. They found that miR-187 was increased in the controls, whereas miR-518f was increased in the osteoporosis group. Neither were identified in our femoral bone biopsies using multivariate analyses.

It is tempting to speculate that mechanically sensitive miRNAs would be associated with BMD and/or fracture, especially in WB femoral bone, but very few of those identified in cell culture studies were associated with BMD or fracture in the current study. A recent study⁽⁹³⁾ identified 10 miRNAs that changed expression when mouse MLOY4 osteocytes were subjected to mechanical strain. However, only two of the identified miRNAs were identified as BMD associated in our study. Of those, miR-29b-3p correlated positively to BMI- and age-adjusted total hip BMD when expressed in both femoral and iliac bone (Fig. S2) but showed reduced expression in MLOY4 cells subjected to mechanical stress. In the same study⁽⁹³⁾ miR-574-3p showed increased expression at mechanical stress, but this miRNA was inversely correlated to BMD when expressed in iliac bone (Table S2). Thus, it is hard to conclude on the association between mechanically sensitive miRNAs and their levels in WB and NWB bone.

Cis-eQTL analyses of iliac bone identified two loci/miRNAs of interest. The locus near the miR-331-3p coding sequence was also identified in the hitherto most comprehensive GWAS on heel eBMD.⁽⁸⁾ However, none of the SNPs identified in the present study were associated with eBMD in the GWAS by Morris and colleagues,⁽⁸⁾ nor were they in LD with any of the eBMD-associated variants.

Morris and colleagues⁽⁸⁾ did not attempt to explain the effect of genomic variation on miRNA expressions but our findings may offer an explanation. Given the biological background of miRNA mechanism of action, an argument can be given for such a nondirect association of miRNA with eBMD variants genomewide based on the present results. Polymorphisms influencing miRNA variation are not influencing BMD variation directly due to epigenetic regulation. It would be desirable to perform a replicate study with a larger cohort, but acquisition of additional biological samples from well-characterized participants will be difficult to obtain.

Most of the BMD-correlated ncRNAs in iliac bone, and in femoral bone, represent novel bone biology. The use of nontraditional statistical methods, such as Lasso, allowed us to select ncRNA sets maximizing the BMD variance explained. The power of this technique was further confirmed by a permutation analysis. This and our previous study⁽¹¹⁾ confine the large number of transcripts expressed in bone biopsies (summing thousands) to a nadir of nine ncRNAs identified through the Lasso analysis and a limited set of mRNAs, which statistically are strongly associated with BMD. These molecular components in bone, as presented in Tables 3 and S4, admittedly at the risk of oversimplification, present an initial schematic outline of an emerging picture of ncRNAs having important roles for normal bone remodeling in NWB iliac bone and WB femoral bone.

Our study has some limitations. The number of participants is limited and the study includes only postmenopausal women of Northwestern European background. Especially for femoral data, power is a limiting factor in terms of the detected number of BMD associated ncRNAs. With a larger cohort, power would be stronger and more BMD associated ncRNA would probably be detected. Nevertheless, our rigorous statistical analyses ensures validity of our findings. The bone biopsies contain marrow, hence the results may be somewhat influenced by transcripts in this tissue. RNA sequencing of the samples indicated that marrow cells of hematopoietic and immunological lineage constituted a minor part (about 20%) of the total cell population contained (not shown). Furthermore, it is expected that marrow constituents across iliac and femoral bone biopsies would be similar. Thus, the detected differences in ncRNA expression between these two sites are most likely attributable to differences in bone cell expression levels. Twenty-two of 46 ncRNAs have been ascribed functional bone cell significance in different experimental systems. Also, the most significantly BMD-correlated miRNAs have been found to be expressed in primary cultured human osteoblasts. We used different platforms for profiling the iliac and femoral bone ncRNAs, but all ncRNAs profiled in iliac bone were covered by microarrays used to profile femoral bone ncRNAs, thus supporting the validity of our findings. Still, we acknowledge that detection methodologies (microarrays with detection of biotin labeled ncRNAs versus TaqMan assays involving detection of PCR products after cleavage of quenching hybridizing probes) and quantification analyses (eg, different types of sample normalization, software, and thresholds) could have an influence on the results. However, several papers show that in general there is a very good concurrence in studies where miRNA levels was measured by both GeneChip miRNA 4.0 Array and TaqMan PCR analysis.^(94–96)

The results invite to a more focused bone transcriptome and functional analyses and thus represent a promising foundation for pursuing studies of miRNAs and other ncRNAs preparing the ground for future gene therapy of a common and devastating disease.

Disclosures

All authors have no conflicts of interest to declare.

Acknowledgments

We are grateful for support from the South-Eastern Norway Regional Health Authority; Oslo University Hospital, Ullevål, project #29750104; the Norwegian Osteoporosis Society; Anders

Jahre Foundation for the Promotion of Science; the Lovisenberg Diaconal Hospital research fund; and the Research Council of Norway. This work is part of the European Union project OSTEOGENE (no. FP6-502491). CM-G and FR are supported by the Netherlands Organization for Health Research and Development (ZonMw VIDI 016.136.367). The present work is dedicated all the Norwegian women who voluntarily participated and made this study possible. We are indebted to the Lovisenberg Diaconal Hospital, Department of Clinical Chemistry for blood sampling and to the hospital's medical outpatient clinic, for access to the surgical facility and patient care assistance. We also acknowledge Diakonhjemmet Hospital, Oslo, for assistance in the collection of femoral bone biopsies. Bioengineer Anne Runningen at The Osteoporosis Laboratory, Lovisenberg Diaconal Hospital, is especially gratefully acknowledged. All primary data are freely available from Dryad (<https://datadryad.org/>).

Authors' roles: KMG and SR designed the study. KMG, VTG, HV, EL, and SR were responsible for patient inclusion and collection of bone biopsies. OKO, LR, VTG, and SR were involved in RNA purification and quantification of bone ncRNAs. CM-C, ES, VP, and FR contributed to the eQTL analysis. C-CG, VP, MH, and SR performed the biostatistical analyses. C-CG, MY, TPU, SR, VP, and KMG contributed to the writing of the manuscript. All authors reviewed the manuscript, added appropriate revisions, agreed to submission for publication, and approved the final version. The corresponding authors attest that all listed authors meet authorship criteria and that no others meeting the criteria have been omitted.

References

- Cooper C. The crippling consequences of fractures and their impact on quality of life. *Am J Med.* 1997;103(2A):125–75.
- Magaziner J, Lydick E, Hawkes W, et al. Excess mortality attributable to hip fracture in white women aged 70 years and older. *Am J Public Health.* 1997;87(10):1630–6.
- Burge R, Dawson-Hughes B, Solomon DH, Wong JB, King A, Tosteson A. Incidence and economic burden of osteoporosis-related fractures in the United States, 2005–2025. *J Bone Miner Res.* 2007;22(3):465–75.
- Jian WX, Long JR, Li MX, Liu XH, Deng HW. Genetic determination of variation and covariation of bone mineral density at the hip and spine in a Chinese population. *J Bone Miner Metab.* 2005;23(2):181–5.
- Sigurdsson G, Halldorsson BV, Styrkarsdottir U, Kristjansson K, Stefansson K. Impact of genetics on low bone mass in adults. *J Bone Miner Res.* 2008;23(10):1584–90.
- Pocock NA, Eisman JA, Hopper JL, Yeates MG, Sambrook PN, Eberl S. Genetic determinants of bone mass in adults. A twin study. *J Clin Invest.* 1987;80(3):706–10.
- Dequeker J, Nijs J, Verstraeten A, Geusens P, Gevers G. Genetic determinants of bone mineral content at the spine and radius: a twin study. *Bone.* 1987;8(4):207–9.
- Morris JA, Kemp JP, Yount SE, et al. An atlas of genetic influences on osteoporosis in humans and mice. *Nat Genet.* 2019;51(2):258–66.
- Lien TG, Borgan O, Reppe S, Gautvik K, Glad IK. Integrated analysis of DNA-methylation and gene expression using high-dimensional penalized regression: a cohort study on bone mineral density in postmenopausal women. *BMC Med Genomics.* 2018;11(1):24.
- Reppe S, Lien TG, Hsu YH, et al. Distinct DNA methylation profiles in bone and blood of osteoporotic and healthy postmenopausal women. *Epigenetics.* 2017;12(8):674–87.
- Reppe S, Refvem H, Gautvik VT, et al. Eight genes are highly associated with BMD variation in postmenopausal Caucasian women. *Bone.* 2010;46(3):604–12.
- Geeleher P, Huang SR, Gamazon ER, Golden A, Seoighe C. The regulatory effect of miRNAs is a heritable genetic trait in humans. *BMC Genomics.* 2012;13:383.
- Liebers R, Rassoulzadegan M, Lyko F. Epigenetic regulation by heritable RNA. *PLoS Genet.* 2014;10(4):e1004296.
- Ying SY, Chang DC, Lin SL. The microRNA (miRNA): overview of the RNA genes that modulate gene function. *Mol Biotechnol.* 2008;38(3):257–68.
- Kozomara A, Griffiths-Jones S. miRBase: annotating high confidence microRNAs using deep sequencing data. *Nucleic Acids Res.* 2014;42(D1):D68–73.
- Cech TR, Steitz JA. The noncoding RNA revolution-trashing old rules to forge new ones. *Cell.* 2014;157(1):77–94.
- Watkins NJ, Bohnsack MT. The box C/D and H/ACA snoRNPs: Key players in the modification, processing and the dynamic folding of ribosomal RNA. *WIREs RNA.* 2012;3(3):397–414.
- Steitz JA, Tycowski KT. Small RNA chaperones for ribosome biogenesis. *Science.* 1995;270(5242):1626–7.
- Kalogeropoulos M, Varanasi SS, Olstad OK, et al. Zic1 transcription factor in bone: neural developmental protein regulates mechanotransduction in osteocytes. *FASEB J.* 2010;24(8):2893–903.
- Varanasi SS, Olstad OK, Swan DC, et al. Skeletal site-related variation in human trabecular bone transcriptome and signaling. *PLoS One.* 2010;5(5):e10692.
- Benjamini Y, Hochberg Y. Controlling the false discovery rate: a practical and powerful approach to multiple testing. *J R Stat Soc Series B Stat Methodol.* 1995;57:289–300.
- Efron B, Hastie T, Johnstone I, Tibshirani R. Least angle regression. *Ann Stat.* 2004;32(2):407–51.
- Friedman J, Hastie T, Tibshirani R. Regularization paths for generalized linear models via coordinate descent. *J Stat Softw.* 2010;33(1):1–22.
- Vlachos IS, Zagganas K, Paraskevopoulou MD, et al. DIANA-miRPath v3.0: deciphering microRNA function with experimental support. *Nucleic Acids Res.* 2015;43(W1):W460–6.
- Alexiou P, Maragkakis M, Papadopoulos GL, Reczko M, Hatzigeorgiou AG. Lost in translation: an assessment and perspective for computational microRNA target identification. *Bioinformatics.* 2009;25(23):3049–55.
- Nielson CM, Liu CT, Smith AV, et al. Novel genetic variants associated with increased vertebral volumetric BMD, reduced vertebral fracture risk, and increased expression of SLC1A3 and EPHB2. *J Bone Miner Res.* 2016;31(12):2085–97.
- Zhan XW, Hu YN, Li BS, Abecasis GR, Liu DJJ. RVTESTS: an efficient and comprehensive tool for rare variant association analysis using sequence data. *Bioinformatics.* 2016;32(9):1423–6.
- De-Ugarte L, Yoskovitz G, Balcells S, et al. MiRNA profiling of whole trabecular bone: identification of osteoporosis-related changes in miRNAs in human hip bones. *BMC Med Genomics.* 2015;8:75.
- Tibshirani R. Regression shrinkage and selection via the Lasso. *J R Stat Soc Series B Stat Methodol.* 1996;58(1):267–88.
- Li Z, Sillanpaa MJ. Overview of LASSO-related penalized regression methods for quantitative trait mapping and genomic selection. *Theor Appl Genet.* 2012;125(3):419–35.
- Hsu YH, Estrada K, Evangelou E, et al. Meta-analysis of genomewide association studies reveals genetic variants for hip bone geometry. *J Bone Miner Res.* 2019;34(7):1284–96.
- Chen J, Long F. mTOR signaling in skeletal development and disease. *Bone Res.* 2018;6:1.
- Shi Y, He G, Lee WC, McKenzie JA, Silva MJ, Long F. Gli1 identifies osteogenic progenitors for bone formation and fracture repair. *Nat Commun.* 2017;8(1):2043.
- Fan JB, Liu W, Zhu XH, et al. EGFR-AKT-mTOR activation mediates epiregulin-induced pleiotropic functions in cultured osteoblasts. *Mol Cell Biochem.* 2015;398(1–2):105–13.
- Manolagas SC. Wnt signaling and osteoporosis. *Maturitas.* 2014;78(3):233–7.

36. Paccou J, Penel G, Chauveau C, Cortet B, Hardouin P. Marrow adiposity and bone: Review of clinical implications. *Bone*. 2019;118:8–15.
37. Hawkes CP, Mostoufi-Moab S. Fat-bone interaction within the bone marrow milieu: impact on hematopoiesis and systemic energy metabolism. *Bone*. 2019;119:57–64.
38. Xiang L, Yu H, Zhang X, et al. The versatile hippo pathway in oral-maxillofacial development and bone remodeling. *Dev Biol*. 2018;440(2):53–63.
39. Lin Z, Tang Y, Tan H, Cai D. MicroRNA-92a-1-5p influences osteogenic differentiation of MC3T3-E1 cells by regulating beta-catenin. *J Bone Miner Metab*. 2019;37(2):264–72.
40. Penzkofer D, Bonauer A, Fischer A, et al. Phenotypic characterization of miR-92a^{-/-} mice reveals an important function of miR-92a in skeletal development. *PLoS One*. 2014;9(6):e101153.
41. Murata K, Ito H, Yoshitomi H, et al. Inhibition of miR-92a enhances fracture healing via promoting angiogenesis in a model of stabilized fracture in young mice. *J Bone Miner Res*. 2014;29(2):316–26.
42. Ahn TK, Kim JO, Kumar H, et al. Polymorphisms of miR-146a, miR-149, miR-196a2, and miR-499 are associated with osteoporotic vertebral compression fractures in Korean postmenopausal women. *J Orthop Res*. 2018;36(1):244–53.
43. Kiss-Laszlo Z, Henry Y, Bachellerie JP, Caizergues-Ferrer M, Kiss T. Site-specific ribose methylation of preribosomal RNA: A novel function for small nucleolar RNAs. *Cell*. 1996;85(7):1077–88.
44. Lestrade L, Weber MJ. snoRNA-LBME-db, a comprehensive database of human H/ACA and C/D box snoRNAs. *Nucleic Acids Res*. 2006;34(Database issue):D158–62.
45. Huttenhofer A, Kieffmann M, Meier-Ewert S, et al. RNomics: an experimental approach that identifies 201 candidates for novel, small, non-messenger RNAs in mouse. *EMBO J*. 2001;20(11):2943–53.
46. Sergiev PV, Aleksashin NA, Chugunova AA, Polikanov YS, Dontsova OA. Structural and evolutionary insights into ribosomal RNA methylation. *Nat Chem Biol*. 2018;14(3):226–35.
47. Ali SA, Zaidi SK, Dobson JR, et al. Transcriptional corepressor TLE1 functions with Runx2 in epigenetic repression of ribosomal RNA genes. *Proc Natl Acad Sci U S A*. 2010;107(9):4165–9.
48. Young DW, Hassan MQ, Pratap J, et al. Mitotic occupancy and lineage-specific transcriptional control of rRNA genes by Runx2. *Nature*. 2007;445(7126):442–6.
49. Ali SA, Zaidi SK, Dacwag CS, et al. Phenotypic transcription factors epigenetically mediate cell growth control. *Proc Natl Acad Sci U S A*. 2008;105(18):6632–7.
50. Parker MS, Balasubramaniam A, Parker SL. The expansion segments of human 28S rRNA down microRNAs much above 18S rRNA or core segments. *Microna*. 2018;7(2):128–37.
51. Verbeeren J, Niemela EH, Turunen JJ, et al. An ancient mechanism for splicing control: U11 snRNP as an activator of alternative splicing. *Mol Cell*. 2010;37(6):821–33.
52. Dupuis-Sandoval F, Poirier M, Scott MS. The emerging landscape of small nucleolar RNAs in cell biology. *Wiley Interdiscip Rev RNA*. 2015;6(4):381–97.
53. Dieci G, Preti M, Montanini B. Eukaryotic snoRNAs: a paradigm for gene expression flexibility. *Genomics*. 2009;94(2):83–8.
54. Kishore S, Gruber AR, Jedlinski DJ, Syed AP, Jorjani H, Zavolan M. Insights into snoRNA biogenesis and processing from PAR-CLIP of snoRNA core proteins and small RNA sequencing. *Genome Biol*. 2013;14(5):R45.
55. Weilner S, Skalicky S, Salzer B, et al. Differentially circulating miRNAs after recent osteoporotic fractures can influence osteogenic differentiation. *Bone*. 2015;79:43–51.
56. Choi YJ, Jeong S, Yoon KA, et al. Deficiency of DGCR8 increases bone formation through downregulation of miR-22 expression. *Bone*. 2017;103:287–94.
57. Liang WC, Fu WM, Wang YB, et al. H19 activates Wnt signaling and promotes osteoblast differentiation by functioning as a competing endogenous RNA. *Sci Rep*. 2016;6:20121.
58. Manochantr S, Marupanthorn K, Tantrawatpan C, Kheolamai P, Tantikanlayaporn D, Sanguanjit P. The effects of BMP-2, miR-31, miR-106a, and miR-148a on osteogenic differentiation of MSCs derived from amnion in comparison with MSCs derived from the bone marrow. *Stem Cells Int*. 2017;2017:7257628.
59. Yavropoulou MP, Anastasilakis AD, Makras P, Tsalikakis DG, Grammatiki M, Yovos JG. Expression of microRNAs that regulate bone turnover in the serum of postmenopausal women with low bone mass and vertebral fractures. *Eur J Endocrinol*. 2017;176(2):169–76.
60. Wang XN, Zhang LH, Cui XD, Wang MX, Zhang GY, Yu PL. lncRNA HOXA11-AS is involved in fracture healing through regulating miR-124-3p. *Eur Rev Med Pharmacol Sci*. 2017;21(21):4771–6.
61. Qadir AS, Um S, Lee H, et al. miR-124 negatively regulates osteogenic differentiation and in vivo bone formation of mesenchymal stem cells. *J Cell Biochem*. 2015;116(5):730–42.
62. Zhao N, Han D, Liu Y, et al. DLX3 negatively regulates osteoclastic differentiation through microRNA-124. *Exp Cell Res*. 2016;341(2):166–76.
63. Chen L, Holmstrom K, Qiu W, et al. MicroRNA-34a inhibits osteoblast differentiation and in vivo bone formation of human stromal stem cells. *Stem Cells*. 2014;32(4):902–12.
64. Hupkes M, Sotoca AM, Hendriks JM, van Zoelen EJ, Decherer KJ. MicroRNA miR-378 promotes BMP2-induced osteogenic differentiation of mesenchymal progenitor cells. *BMC Mol Biol*. 2014;15(1):1–15.
65. Kahai S, Lee SC, Lee DY, et al. MicroRNA miR-378 regulates nephron expression modulating osteoblast differentiation by targeting GalNT-7. *PLoS One*. 2009;4(10):e7535.
66. You L, Gu W, Chen L, Pan L, Chen J, Peng Y. MiR-378 overexpression attenuates high glucose-suppressed osteogenic differentiation through targeting CASP3 and activating PI3K/Akt signaling pathway. *Int J Clin Exp Pathol*. 2014;7(10):7249–61.
67. Zeng HC, Bae Y, Dawson BC, et al. MicroRNA miR-23a cluster promotes osteocyte differentiation by regulating TGF-beta signalling in osteoblasts. *Nat Commun*. 2017;8:15000.
68. Gu C, Xu Y, Zhang S, et al. miR-27a attenuates adipogenesis and promotes osteogenesis in steroid-induced rat BMSCs by targeting PPAR-gamma and GREM1. *Sci Rep*. 2016;6:38491.
69. You L, Pan L, Chen L, Gu W, Chen J. MiR-27a is essential for the shift from osteogenic differentiation to adipogenic differentiation of mesenchymal stem cells in postmenopausal osteoporosis. *Cell Physiol Biochem*. 2016;39(1):253–65.
70. Gong Y, Lu J, Yu X, Yu Y. Expression of Sp7 in Satb2-induced osteogenic differentiation of mouse bone marrow stromal cells is regulated by microRNA-27a. *Mol Cell Biochem*. 2016;417(1–2):7–16.
71. Van Metre TE Jr, Marsh DG, Adkinson NF Jr, et al. Immunotherapy for cat asthma. *J Allergy Clin Immunol*. 1988;82(6):1055–68.
72. Huang M, Qing Y, Shi Q, Cao Y, Song K. miR-342-3p elevates osteogenic differentiation of umbilical cord mesenchymal stem cells via inhibiting Sufu in vitro. *Biochem Biophys Res Commun*. 2017;491(3):571–7.
73. Guo Y, Tang CY, Man XF, et al. Insulin receptor substrate-1 time-dependently regulates bone formation by controlling collagen lpha2 expression via miR-342. *FASEB J*. 2016;30(12):4214–26.
74. Vimalraj S, Partridge NC, Selvamurugan N. A positive role of microRNA-15b on regulation of osteoblast differentiation. *J Cell Physiol*. 2014;229(9):1236–44.
75. Gao J, Yang T, Han J, et al. MicroRNA expression during osteogenic differentiation of human multipotent mesenchymal stromal cells from bone marrow. *J Cell Biochem*. 2011;112(7):1844–56.
76. Xu C, Zhang H, Gu W, et al. The microRNA-10a/ID3/RUNX2 axis modulates the development of ossification of posterior longitudinal ligament. *Sci Rep*. 2018;8(1):9225.
77. Deng L, Hu G, Jin L, Wang C, Niu H. Involvement of microRNA-23b in TNF-alpha-reduced BMSC osteogenic differentiation via targeting runx2. *J Bone Miner Metab*. 2018;36(6):648–60.
78. Waki T, Lee SY, Niikura T, et al. Profiling microRNA expression during fracture healing. *BMC Musculoskelet Disord*. 2016;17:83.
79. Bhushan R, Grunhagen J, Becker J, Robinson PN, Ott CE, Knaus P. miR-181a promotes osteoblastic differentiation through repression of TGF-beta signaling molecules. *Int J Biochem Cell Biol*. 2013;45(3):696–705.

80. Okamoto H, Matsumi Y, Hoshikawa Y, Takubo K, Ryoke K, Shiota G. Involvement of microRNAs in regulation of osteoblastic differentiation in mouse induced pluripotent stem cells. *PLoS One*. 2012;7(8): e43800.
81. Reppe S, Noer A, Grimholt RM, et al. Methylation of bone SOST, its mRNA, and serum sclerostin levels correlate strongly with fracture risk in postmenopausal women. *J Bone Miner Res*. 2015;30(2):249–56.
82. Lee EJ, Kim SM, Choi B, et al. Interleukin-32 gamma stimulates bone formation by increasing miR-29a in osteoblastic cells and prevents the development of osteoporosis. *Sci Rep*. 2017;7:40240.
83. Kapinas K, Kessler CB, Delany AM. miR-29 suppression of osteonectin in osteoblasts: regulation during differentiation and by canonical Wnt signaling. *J Cell Biochem*. 2009;108(1):216–24.
84. Ko JY, Chuang PC, Ke HJ, Chen YS, Sun YC, Wang FS. MicroRNA-29a mitigates glucocorticoid induction of bone loss and fatty marrow by rescuing Runx2 acetylation. *Bone*. 2015;81:80–8.
85. Roberto VP, Tiago DM, Silva IA, Cancela ML. MiR-29a is an enhancer of mineral deposition in bone-derived systems. *Arch Biochem Biophys*. 2014;564:173–83.
86. Kapinas K, Kessler C, Ricks T, Gronowicz G, Delany AM. miR-29 modulates Wnt signaling in human osteoblasts through a positive feed-back loop. *J Biol Chem*. 2010;285(33):25221–31.
87. Dernowsek JA, Pereira MC, Fornari TA, et al. Posttranscriptional interaction between miR-450a-5p and miR-28-5p and STAT1 mRNA triggers osteoblastic differentiation of human mesenchymal stem cells. *J Cell Biochem*. 2017;118(11):4045–62.
88. Zhang L, Tang Y, Zhu X, et al. Overexpression of MiR-335-5p promotes bone formation and regeneration in mice. *J Bone Miner Res*. 2017;32(12):2466–75.
89. Jeong BC, Kang IH, Hwang YC, Kim SH, Koh JT. MicroRNA-194 reciprocally stimulates osteogenesis and inhibits adipogenesis via regulating COUP-TFII expression. *Cell Death Dis*. 2014;5:e1532.
90. Huang X, Li D, Wang Z, et al. Study of microRNAs targeted Dvl2 on the osteoblasts differentiation of rat BMSCs in hyperlipidemia environment. *J Cell Physiol*. 2018;233(9):6758–66.
91. Seeliger C, Karpinski K, Haug AT, et al. Five freely circulating miRNAs and bone tissue miRNAs are associated with osteoporotic fractures. *J Bone Miner Res*. 2014;29(8):1718–28.
92. Garmilla-Ezquerria P, Sanudo C, Delgado-Calle J, Perez-Nunez MI, Sumillera M, Riancho JA. Analysis of the bone microRNome in osteoporotic fractures. *Calcif Tissue Int*. 2015;96(1):30–7.
93. Zeng Q, Wang Y, Gao J, et al. miR-29b-3p regulated osteoblast differentiation via regulating IGF-1 secretion of mechanically stimulated osteocytes. *Cell Mol Biol Lett*. 2019;24:11.
94. Oshima G, Poli EC, Bolt MJ, et al. DNA methylation controls metastasis-suppressive 14q32-encoded miRNAs. *Cancer Res*. 2019;79(3):650–62.
95. Huang H, Zhang C, Wang B, et al. Transduction with lentiviral vectors altered the expression profile of host microRNAs. *J Virol*. 2018;92(18): e00503-18.
96. Jung DE, Park SB, Kim K, Kim C, Song SY. CG200745, an HDAC inhibitor, induces anti-tumour effects in cholangiocarcinoma cell lines via miRNAs targeting the Hippo pathway. *Sci Rep*. 2017;7(1):10921.